Rapid coherent control of population transfer in lattice systems

Shumpei Masuda[1,2,*] and Stuart A. Rice[1]
[1]*The James Franck Institute, The University of Chicago, Chicago, Illinois 60637, USA*
[2]*Department of Physics, Tohoku University, Sendai 980, Japan*
(Received 8 November 2013; revised manuscript received 10 February 2014; published 14 March 2014)

We derive the driving potential that accelerates adiabatic population transfer from an initial state to a target state in a lattice system without unwanted excitation of other states by extending to discrete systems the fast-forward theory of adiabatic transfer. As an example, we apply the theory to a model that describes a Bose-Einstein condensate in a quasi-one-dimensional optical lattice, and show that modulation of the tilting of the lattice potential can transfer the population of the Bose-Einstein condensate from site to site with high fidelity and without unwanted excitations.

DOI: 10.1103/PhysRevA.89.033621 PACS number(s): 67.85.−d, 02.30.Yy, 37.10.Jk

I. INTRODUCTION

During the past three decades there have been dramatic advances in both theoretical understanding of the requirements for control of quantum dynamics and the technology that is needed for the execution of proposed control paradigms [1,2]. Experimental verifications of the theory for systems as diverse as control of population transfer in Bose-Einstein condensates (BECs) and in chemical reactions have been reported [3–10]. A particularly useful subgroup of the proposals for control of quantum dynamics of a system rely on adiabatic transfer via the slow variation of an external field that is applied to the system. However, experimental exploitation of such control schemes can be rendered difficult by the occurrence of unwanted internal decoherence processes and by external noise; both of these difficulties can be reduced or avoided if the adiabatic transfer process can be speeded up sufficiently to permit population transfer to compete successfully with the time dependence of the perturbations. Indeed, with this goal in mind, several methods for the acceleration of quantum dynamics, including adiabatic dynamics, have been proposed. These methods include the counterdiabatic protocol [11], frictionless quantum driving [12,13], invariant-based inverse engineering [14], and fast-forward scaling [15–19], which is also used for protection of quantum states from potential fluctuations [20].

Lattice models of quantum systems, examples of which are a BEC in an optical lattice, a network of nonlinear wave guides and optical fibers, and a superconducting ladder of Josephson junctions, are widely exploited. Thus motivated by the potential applicability to quantum computation, and by the opportunity to simulate aspects of complex electronic behavior in crystalline matter, many remarkable features of BECs in optical lattices have been studied [21]. The existing studies clearly reveal the value of the ability to manipulate BECs in optical lattices for the purpose of preparing well-defined quantum states. We have been stimulated by this observation to extend the theory of accelerated adiabatic transfer to lattice systems so as to determine the potential that drives specified state-to-state population transfer without excitation of unwanted quantum states. Our approach differs from that of Liew and Shelykh [22] who studied interwell population transfer in the nonadiabatic regime generated by a laser pulse with preselected shape. Their numerical analysis, which is based on a discrete nonlinear Schrödinger equation, varies the pulse parameters to optimize the fidelity of the population transfer. Our approach is analytic; we provide a derivation of the potential that drives population transfer from site to site, and we apply the theory to a BEC in a quasi-one-dimensional optical lattice. We show that modulation of the lattice potential can transfer the population of the BEC between sites of the lattice with high fidelity and without unwanted excitations. The theory developed is applicable to any lattice in which the on-site potential is tunable. We also demonstrate the robustness of the accelerated population transfer to variation (approximation) of the driving potential.

In Sec. II we present the framework of the theory of accelerated quantum adiabatic dynamics in a lattice system and discuss its relationship with the corresponding theory for a continuous system. In Sec. III we study accelerated population transfer in a Bose-Einstein condensate in a one-dimensional optical lattice potential. The robustness of the method with respect to approximation of the driving potential is studied in Sec. IV. An Appendix provides a brief description of the basic theory of acceleration of nonadiabatic quantum dynamics.

II. FAST-FORWARD TRANSFORMATION IN DISCRETE SYSTEMS

We consider a lattice system in which the dynamics is governed by a discrete time-dependent Schrödinger equation,

$$i\frac{d\Psi(m,t)}{dt} = \sum_l \omega_{m,l}\Psi(l,t) + \frac{V_0(m,R(t))}{\hbar}\Psi(m,t), \quad (1)$$

where l,m denote sites and t time, respectively, and $\omega_{m,l} = \omega^*_{l,m}$ is the rate of hopping between sites m and l. The potential V_0 is modulated by a parameter R, which is a function of t. If the parameter R changes slowly enough from R_i to R_f, and if the initial state is the nth energy eigenstate of the Hamiltonian with potential $V_0(R_i)$, the wave function of the state on site m changes from $\phi_n(m,R_i)$ to $\phi_n(m,R_f)$ modulo the dynamical and adiabatic phases of the states. The wave function $\phi_n(m,R)$

*masuda@uchicago.edu

is a solution of the time-independent Schrödinger equation,

$$\sum_l \hbar\omega_{m,l}\phi_n(l,R) + V_0(m,R)\phi_n(m,R) = E_n(R)\phi_n(m,R). \quad (2)$$

On the other hand, when the parameter R changes at a nonzero rate, transitions occur to other levels. Our purpose is to derive a potential that drives the state from $\phi_n(m,R_i)$ to $\phi_n(m,R_f)$ in some short time T_F without unwanted excitations to other states. For that purpose we consider an intermediate state whose wave function is represented as

$$\Psi_{\rm FF}(m,t) = \phi_n(m,R(t))\exp[if(m,t)] \times \exp\left[-\frac{i}{\hbar}\int_0^t E_n(R(t'))dt'\right]. \quad (3)$$

Note that Eq. (3) contains the additional phase $f(m,t)$, and that the intermediate state connects the initial state $\phi_n(m,R_i)$ and the target state $\phi_n(m,R_f)\exp[-\frac{i}{\hbar}\int_0^{T_F} E_n(R(t'))dt']$ in time T_F. We require that this additional phase vanishes at $t=0$ and at $t=T_F$, and we assume that the intermediate state satisfies the time-dependent Schrödinger equation

$$i\frac{d\Psi_{\rm FF}(m,t)}{dt} = \sum_l \omega_{m,l}\Psi_{\rm FF}(l,t) + \frac{V_{\rm FF}(m,t)}{\hbar}\Psi_{\rm FF}(m,t), \quad (4)$$

in which $V_{\rm FF}(m,t)$ is the driving potential. We seek the driving potential that generates $\phi_n(m,R_f)\exp[-\frac{i}{\hbar}\int_0^{T_F} E_n(R(t'))dt']$ from $\phi_n(m,R_i)$. Although we do not aim to generate the adiabatic phase, that uniform phase can be tuned by a uniform potential if necessary.

To find the forms of the driving potential and the additional phase $f(m,t)$ we substitute Eq. (3) into the Schrödinger equation (4) and we use Eq. (2) to rearrange the resulting equation. The imaginary part of the resultant equation leads to

$$\dot{R}\,{\rm Re}\{\phi_n^*(m,R)\partial_R\phi_n(m,R)\} = \sum_l {\rm Im}(\omega_{m,l}\phi_n^*(m,R)\phi_n(l,R) \times \{\exp[i(f(l,t)-f(m,t))]-1\}). \quad (5)$$

The solution of Eq. (5) yields the additional phase $f(m,t)$, and the real part gives the driving potential as a functional of f, V_0, R, and ϕ_n:

$$V_{\rm FF}(m,t) = V_0(m,R(t)) + \sum_l {\rm Re}\left\{\hbar\omega_{m,l}\frac{\phi_n(l,R(t))}{\phi_n(m,R(t))} \times (1-\exp[i\{f(l,t)-f(m,t)\}])\right\} - \hbar\dot{f}(m,t) - \hbar\dot{R}\,{\rm Im}\left[\frac{\partial_R\phi_n(m,R(t))}{\phi_n(m,R(t))}\right]. \quad (6)$$

It is necessary that R satisfies the conditions

$$R(0) = R_i, \qquad R(T_F) = R_f. \quad (7)$$

If we take the boundary conditions to be

$$\dot{R}(0) = \dot{R}(T_F) = 0, \quad (8)$$

$f(m,t)$ vanishes at $t=0$ and at $t=T_F$ [see Eq. (5)], and the intermediate state coincides with the target state at T_F. The driving potential is obtained by substituting the additional phase into Eq. (6). With the boundary conditions

$$\ddot{R}(0) = \ddot{R}(T_F) = 0, \quad (9)$$

the driving potential coincides with V_0 at $t=0$ and at $t=T_F$. The time dependence of R is arbitrary except for the requirement imposed by the above boundary conditions. The driving potential depends on the time dependence of R.

In the case that the hopping rate and the wave function are real, Eqs. (5) and (6) simplify to

$$\dot{R}\partial_R\phi_n(m,R) = \sum_l \omega_{m,l}\phi_n(l,R)\sin[f(l,t)-f(m,t)] \quad (10)$$

and

$$V_{\rm FF}(m,t) = V_0(m,R(t)) + \sum_l \hbar\omega_{m,l}\frac{\phi_n(l,R(t))}{\phi_n(m,R(t))} \times\{1-\cos[f(l,t)-f(m,t)]\} - \hbar\dot{f}(m,t). \quad (11)$$

We note that Eq. (5) implies that for $\dot{R}$ sufficiently large there is no solution for $f(m,t)$. That is, there is a lower limit to the control time T_F. This property is not seen in the fast-forward theory for continuous systems [16]. Equations (5) and (6), for f and for $V_{\rm FF}$, reduce to the corresponding equations for continuous systems shown in Ref. [16] in the limit that the differences between adjacent sites of f and of ϕ_n are small. The theory of acceleration of nonadiabatic quantum dynamics in a continuous system is described in Ref. [15]. Following the same analysis as in Ref. [15], the key elements of the theory of accelerated nonadiabatic quantum dynamics in a lattice system are exhibited in the Appendix.

The analysis described above can be straightforwardly extended to the case when a nonlinear Schrödinger equation is the basic descriptor of the system dynamics. Consider

$$i\frac{d\Psi(m,t)}{dt} = \sum_l \omega_{m,l}\Psi(l,t) + \frac{V_0(m,R(t))}{\hbar}\Psi(m,t) + \frac{c}{\hbar}|\Psi(m,t)|^2\Psi(m,t), \quad (12)$$

where c is a constant. We assume the same form of the wave function for the intermediate state $\Psi_{\rm FF}$ as in Eq. (3). Then ϕ_n is a solution of the time-independent nonlinear Schrödinger equation,

$$\sum_l \hbar\omega_{m,l}\phi_n(l,R) + V_0(m,R)\phi_n(m,R) + c|\phi_n(m,R)|^2\phi_n(m,R) = E_n(R)\phi_n(m,R). \quad (13)$$

We assume that the intermediate-state wave function is defined by the nonlinear Schrödinger equation

$$i\frac{d\Psi_{\rm FF}(m,t)}{dt} = \sum_l \omega_{m,l}\Psi_{\rm FF}(l,t) + \frac{V_{\rm FF}}{\hbar}(m,t)\Psi_{\rm FF}(m,t) + \frac{c}{\hbar}|\Psi_{\rm FF}(m,t)|^2\Psi_{\rm FF}(m,t). \quad (14)$$

We can derive the equations for the additional phase and the driving potential in the same manner as for the linear

Schrödinger equation. The resultant equations are the same as Eqs. (5) and (6), respectively. The nonlinear term influences the driving potential through ϕ_n in Eq. (13).

III. SITE-TO-SITE POPULATION TRANSFER OF A BEC IN AN OPTICAL LATTICE

As an example, we now consider driving site-to-site population transfer of a BEC in an optical lattice. The lattice is defined by an external potential that is the sum of a spatially linear potential, which is tunable, and a stationary periodic potential

$$V_{\rm ext}(\mathbf{r},t) = \xi(t)z + U_L(x,y)\sin^2(2\pi z/\lambda), \tag{15}$$

where $\lambda/2$ is the wavelength (period) of the potential. A discrete model of the BEC in a tilted (washboard) periodic trap was introduced in Ref. [23], using the tight-binding approximation. In the tight-binding approximation the condensate order parameter is written as [23,24]

$$\Phi(\mathbf{r},t) = \sqrt{N_T}\sum_m \Psi(m,t)\varphi(\mathbf{r}-\mathbf{r}_m), \tag{16}$$

where N_T is the total number of atoms and $\varphi(m,\mathbf{r}) = \varphi(\mathbf{r}-\mathbf{r}_m)$ is the condensate wave function localized in the mth trap with location $\mathbf{r}_m$ and $\int \varphi^2(m,\mathbf{r})d\mathbf{r} = 1$. The tight-binding approximation is based on the assumption that the interwell barriers are much higher than the chemical potential [23,24]. The wave function $\varphi(m,\mathbf{r})$ overlaps in the barrier region with the wave functions $\varphi(m\pm1,\mathbf{r})$ in the neighboring sites. Because the barrier is high, the overlap is much smaller than 1, $\int \varphi(m,\mathbf{r})\varphi(m+1,\mathbf{r})d\mathbf{r} \simeq 0$. We also assume that the energy of the system is confined within the lowest band. The validity of this model has been confirmed by comparing numerical results with experimental results in Ref. [24]. Using Eq. (16), the Gross-Pitaevskii equation can be rewritten to read [23]

$$i\hbar\frac{\partial}{\partial t}\Psi(m,t) = -K[\Psi(m-1,t)+\Psi(m+1,t)] + \frac{\xi(t)\lambda m}{2}\Psi(m,t) + c'|\Psi(m,t)|^2\Psi(m,t), \tag{17}$$

where

$$K \simeq -\int d\mathbf{r}\left[\frac{\hbar^2}{2m_0}\nabla\varphi(m,\mathbf{r})\cdot\nabla\varphi(m+1,\mathbf{r}) + \varphi(m,\mathbf{r})V_{\rm ext}(\mathbf{r})\varphi(m+1,\mathbf{r})\right], \tag{18}$$

$$c' \simeq gN_T\int d\mathbf{r}|\varphi(m,\mathbf{r})|^4, \tag{19}$$

with m_0 the mass of an atom, $g(=4\pi\hbar^2 a/m_0)$ the coupling constant, a the scattering length, and N_T the total number of atoms. Since the lattice potential is high in the region where the wave functions $\varphi(m,\mathbf{r})$ and $\varphi(m+1,\mathbf{r})$ overlap, it contributes to K much more than does the linear spatial potential, and we can neglect the m dependence of K. Equation (17) then can be rewritten as

$$i\frac{\partial}{\partial t}\Psi(m,t) = \tilde{\omega}[\Psi(m-1,t)+\Psi(m+1,t)] + \frac{V(m,t)}{\hbar}\Psi(m,t) + \frac{c'}{\hbar}|\Psi(m,t)|^2\Psi(m,t), \tag{20}$$

with

$$\tilde{\omega} = -K/\hbar \tag{21}$$

and

$$V(m,t) = \tfrac{1}{2}\xi(t)\lambda m. \tag{22}$$

We demonstrate the acceleration of population transfer for a BEC in a lattice with this model. Our goal is the transfer of population to the ground state of the linear potential with $\xi = \xi_f$ from the ground state of the linear potential with $\xi = \xi_i$. We take $\xi_i = -\xi_f$ so that the population is transferred from one side of the lattice to the opposite side of the lattice.

A. Three-site model

We consider first a three-site model with site potential

$$V_0(m,R(t)) = \hbar\omega R(t)m. \tag{23}$$

In Eq. (23), the constant frequency ω is defined by

$$\omega = -\frac{\xi_i\lambda}{2\hbar} = \frac{\xi_f\lambda}{2\hbar}, \tag{24}$$

and the time dependence of $R(t)$ is chosen to be

$$R(t) = R_0 + \frac{2}{T_F}\left[t - \frac{T_F}{2\pi}\sin\left(\frac{2\pi}{T_F}t\right)\right]. \tag{25}$$

We take $R_0 = -1$, so that $V_0(m,R(t))$ changes from $\xi_i\lambda m/2$ to $\xi_f\lambda m/2$ in time T_F, and take the hopping rate in Eq. (1) to be

$$\omega_{m,l} = \tilde{\omega}(\delta_{m,l-1}+\delta_{m,l+1}). \tag{26}$$

We have calculated the additional phase and driving potential for this model system using Eqs. (10) and (11), respectively, with the parameter set $T_F = 4.2$ ms, $\omega = 2.14$ [1/ms], $\hbar/(2K) = 0.35$ ms, $c' = 0$, and $\lambda = 850$ nm [23]. The effect of finite nonlinear constant ($c' > 0$) is studied in Sec. IV. The trap depths, which scale linearly with the intensity of the beam, are $1.4E_R$ at the center of the beam with $E_R = \hbar^2k^2/(2m_0)$ and $k = 2\pi/\lambda$. m_0 is taken to be the mass of ^{87}Rb. The time dependence of the additional phase is shown in Fig. 1, where we choose $f(1,t) = 0$. The driving potential $V_{\rm FF}(m,t)$, shown in Fig. 2, differs from $V_0(m,R(t))$ for $0 < t < T_F$, and is equal to V_0 at $t = 0$ and $t = T_F$. We have simulated the evolution of the model system driven by $V_{\rm FF}(m,t)$ from the ground state corresponding to $V_0(m,R(0))$. That evolution is monitored by the fidelity

$$F(t) = |\langle\phi_0|\Psi\rangle|, \tag{27}$$

where $|\phi_0\rangle$ is the ground state of the instantaneous Hamiltonian $H_0(R(t))$ and $|\Psi\rangle$ is the state driven by the potential $V_{\rm FF}(m,t)$. The time dependence of the fidelity is shown in the inset to Fig. 2; it is equal to unity at T_F. A comparison of the population evolution under $V_0(m,R(t))$ and under $V_{\rm FF}(m,t)$

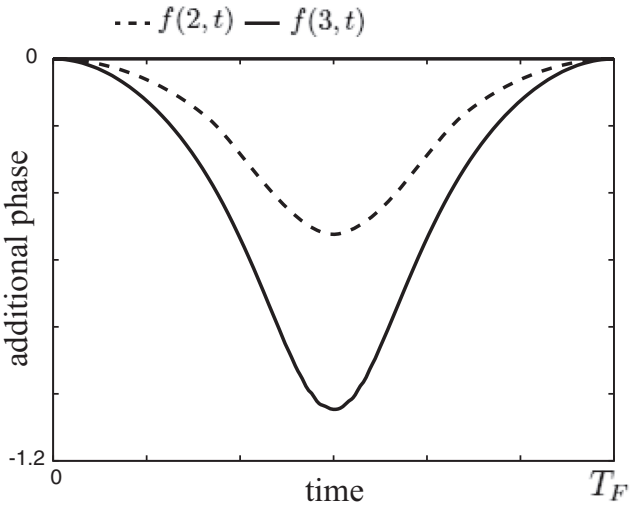

FIG. 1. Time dependence of the additional phase.

is shown in Fig. 3. We note that the nonadiabatic transfer generates unwanted excitations, with the population of each site deviating from that evolving under the instantaneous Hamiltonian (dotted lines in Fig. 3). The fidelity of the population evolution driven by $V_0(m,R(t))$ is 0.938 at T_F.

B. Four-site model

We have also examined accelerated population transfer of a BEC in a four-site model. The parameters used for these calculations are the same as for the three-site model except that $\omega = 0.714$ [1/ms]. The population of the ground state of the instantaneous Hamiltonian for each site is shown in Fig. 4. The initial state is located mainly at sites 3 and 4, while the target state is located mainly at sites 1 and 2. The time dependence of the driving potential is shown in Fig. 5. The time dependence

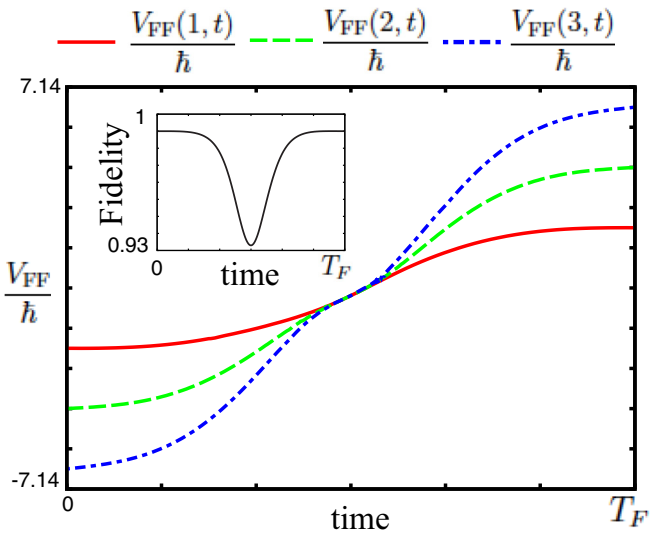

FIG. 2. (Color online) Time dependence of $V_{FF}(m,t)/\hbar$. The unit of time is 1 ms. The inset shows the time dependence of the fidelity, defined by $F(t) = |\langle\phi_0|\Psi\rangle|$.

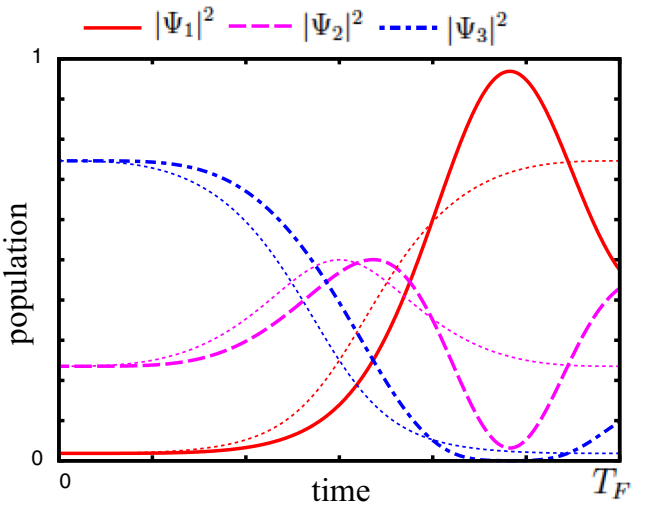

FIG. 3. (Color online) Time dependence of the population evolution under $V_0(m,R(t))$ (dashed and solid lines) and $V_{FF}(m,t)$ (dotted lines). The evolution under the instantaneous Hamiltonian is also shown with dotted lines. The notation is $\Psi_m = \Psi(m,t)$.

of the fidelity is compared in the inset to Fig. 5. The solid curve and the broken curve correspond to the dynamics with V_{FF} and V_0, respectively. We note that the fidelity decreases and does not recover at T_F in the V_0 generated dynamics because of unwanted excitations, whereas for the V_{FF} generated dynamics the fidelity becomes unity at $t = T_F$.

IV. COMMENTS

It is one matter to calculate the exact driving potential that is required for transfer of the BEC population between lattice sites with perfect fidelity, but it is another matter to generate that potential in a real experiment. We consider two limiting cases.

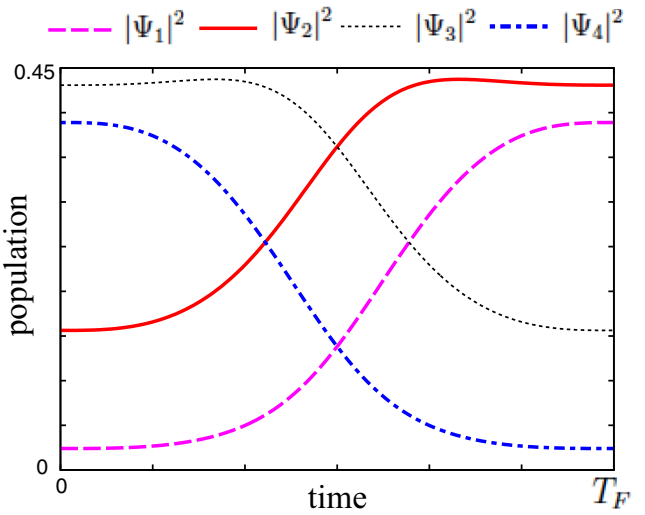

FIG. 4. (Color online) Population of the ground state of the instantaneous Hamiltonian in the four-site model system.

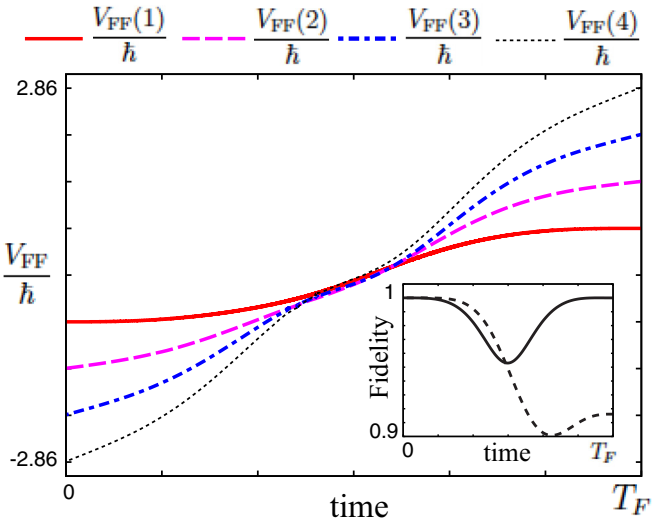

FIG. 5. (Color online) Time dependence of $V_{FF}(i,t)/\hbar$. The unit of time is 1 ms. The inset shows the time dependence of the fidelity.

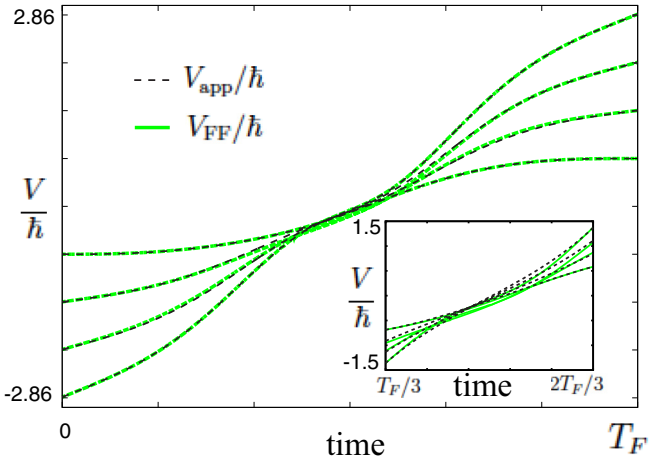

FIG. 6. (Color online) Comparison of $V_{app}/\hbar$ and $V_{FF}/\hbar$. The unit of the vertical axis is 1 [1/ms]. The inset shows the time dependence of $V/\hbar$ for $T_F/3 \leqslant t \leqslant 2T_F/3$.

First, it is usually the case that in real experiments we cannot generate a perfect rendition of a specified potential. Then, testing the robustness of the proposed population transfer method to deviation from the exact driving potential is important. We test the efficiency of our proposed transfer process to approximation of the driving potential by considering population transfer under a driving potential that is proportional to the site number:

$$V_{app}(j,t) = \mathcal{V}(t)\, j. \tag{28}$$

In Eq. (28), $\mathcal{V}(t)$ is a function designed so that V_{app} approximates the exact driving potential. For the three-site model with $c' = 0$, for transfers between ground states, V_{app} coincides with V_{FF} because

$$\begin{aligned}&\phi_n(1,R)\left[2\phi_n^2(3,R) - \phi_n^2(2,R)\right] \\ &\quad = \phi_n(3,R)\left[\phi_n^2(2,R) - 2\phi_n^2(1,R)\right],\end{aligned} \tag{29}$$

for any R. This property also holds for the second and third eigenstates of the instantaneous Hamiltonian, although the driving potential depends on the level n. Thus the simple potential defined in Eq. (28) can transfer population in the three-site model without unwanted excitation if $c' = 0$. The approximation $V_{app}(j,t) = \mathcal{V}(t)\, j$ is not exact for the four-site model or the three-site model with $c' \neq 0$, but it is a good approximation to V_{FF} for those models. We show the difference between V_{app} and V_{FF} for the four-site model with $c' = 0$ in Fig. 6. In general, V_{FF} is well approximated by V_{app} with a larger deviation near $t = T_F/2$ than in other time domains (the inset of Fig. 6). The fidelity of the population transfer in the four-site system driven by V_{app} is 0.9997 at T_F, whilst the fidelity of the population transfer driven by V_0 is 0.916. The time dependence of $\mathcal{V}(t)/\hbar$ for $c'/\hbar = \{0, 1.43, 4.29\}$ [1/ms] is compared with $\omega R(t)$ in Fig. 7. The values of c' used here are in the range of that used in Ref. [23]. For $c'/\hbar = 1.43$ and 4.29 [1/ms] the fidelity at $t = T_F$ of the V_{app} driven dynamics is 0.9998 and 0.999 94, respectively, whilst in the V_0 driven dynamics $F(T_F) = 0.9482$ and 0.9772, respectively. For large c' the difference between $\mathcal{V}(t)/\hbar$ and $\omega R(t)$ is small, because the wave function $\phi_n(m)$ flattens with respect to m for $c' > 0$, and the variance of the wave function during the control is smaller than that when $c' = 0$. This property makes the additional phase $f(m)$ flatten and the variance of the additional phase is small during the dynamics. Therefore, the second and the third terms in Eq. (11) are small for large c'.

Second, in real experiments, we cannot know the on-site potential $V_0(m)$ or the hopping rate $\omega_{m,l}$, exactly. To model this uncertainty we consider the three-site model with (a) an on-site potential with deviation from the nominal potential of $\delta V(m)$ and (b) a hopping rate with deviation from the nominal value of $\delta\omega_{m,l}$. The other parameters are taken to be the same as used for the calculation shown in Fig. 2 except for c'. To determine the sensitivity of the fidelity to the deviations $\delta V(m)$ and $\delta\omega_{m,l}$, the approximated driving potential, $V_{app}(m,t)$, is calculated for the system with nonzero values of $\delta V(m)$ or $\delta\omega_{m,l}$. However, the initial and the target states are taken to be

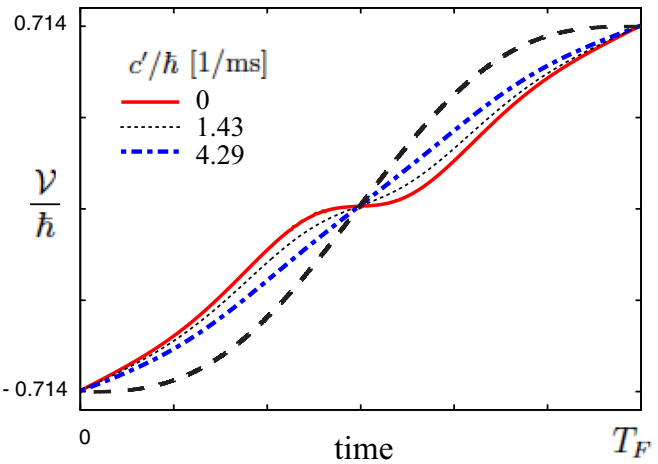

FIG. 7. (Color online) Comparison of $\mathcal{V}(t)/\hbar$ for $c'/\hbar = \{0, 1.43, 4.29\}$ [1/ms] and $\omega R(t)$ (black broken curve). The unit of the vertical axis is 1 [1/ms].

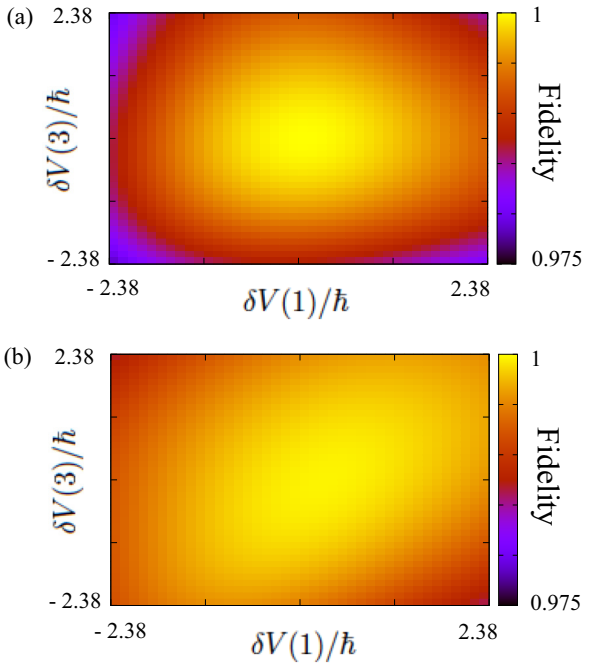

FIG. 8. (Color online) Dependence of the fidelity at T_F on $\delta V(1)/\hbar$ and $\delta V(3)/\hbar$ for $\delta V(2) = 0$ with $c'/\hbar = 0$ (upper panel) and 1.43 [1/ms] (lower panel). The unit of time is 1 ms.

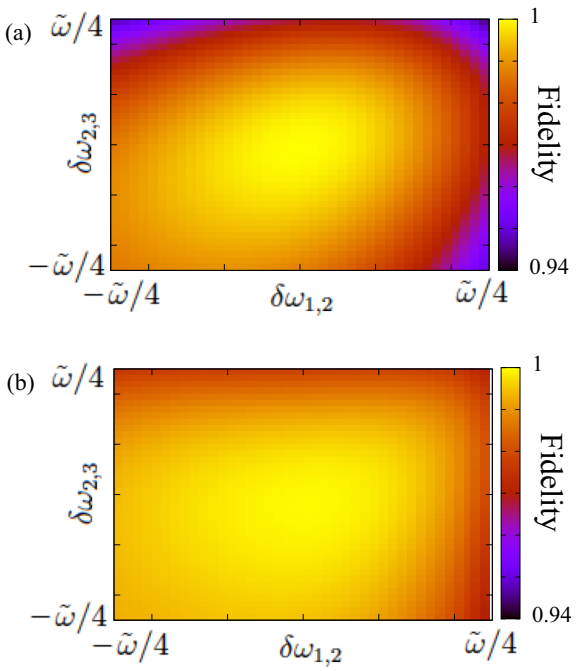

FIG. 9. (Color online) Dependence of the fidelity at T_F on $\delta\omega_{1,2}$ and $\delta\omega_{2,3}$ for $c'/\hbar = 0$ (upper panel) and 1.43 [1/ms] (lower panel).

the ground states of the instantaneous Hamiltonian with $\delta V(m)$ and $\delta\omega_{m,l} = 0$. The fidelity is calculated with the ground state of the instantaneous Hamiltonian.

In Fig. 8 we display the fidelity as a function of $\delta V(1)/\hbar$ and $\delta V(3)/\hbar$ for the case $\delta V(2)/\hbar = 0$, $c'/\hbar = 0$, and 1.43 [1/ms]. In the range of $\delta V(m)$ used the maximum value is $V_0(1, R_{\rm fin})/3$; the fidelity $F(T_F)$ is larger than that of the population evolution driven by $V_0(m, R(t))$ without potential uncertainty, $F(T_F) = 0.938$ for $c'/\hbar = 0$, and $F(T_F) = 0.9723$ for $c'/\hbar = 1.43$ [1/ms]. In spite of the fact that $V_{\rm app} \neq V_{\rm FF}$ for $c' \neq 0$, our control for $c'/\hbar = 1.43$ [1/ms] is more robust than that for $c' = 0$, because the wave function $\phi_n(m)$ flattens with respect to m for $c' > 0$, and the variance of the wave function during the control is smaller than that when $c' = 0$. $F(T_F) > 0.998$ for $c'/\hbar = 4.29$ [1/ms] in the range of $\delta V(m)$ used.

In Fig. 9 we show the dependence of the fidelity on $\delta\omega_{m,l}$ with the hopping rate taken to be

$$\omega_{1,2} = \tilde{\omega} + \delta\omega_{1,2}, \qquad \omega_{2,3} = \tilde{\omega} + \delta\omega_{2,3}. \tag{30}$$

In the range of $\delta\omega_{m,l}$ used the maximum value of $|\delta\omega_{m,l}|$ is $\tilde{\omega}/4$. In this range the fidelity $F(T_F)$ is larger than that of the population evolution driven by $V_0(m, R(t))$ without uncertainty of the hopping rate. The control for $c'/\hbar = 1.43$ [1/ms] is more robust with respect to $\delta\omega_{m,l}$ than that for $c'/\hbar = 0$. $F(T_F) > 0.988$ for $c'/\hbar = 4.29$ [1/ms] in the range of $\delta\omega_{m,l}$ used.

The tight-binding approximation with the wave function displayed in Eq. (16) is based on the assumption that the energy of the system is confined within the lowest band. The band gap is about $3U/5$ [24], where U is the barrier height. The maximum potential difference between the left-hand and right-hand lattice sites is about $0.15U$ for the three-site model and $0.075U$ for the four-site model; hence the potential difference between the left-hand and right-hand sites of our model is less than the band gap throughout the period of time that we drive the population transfer.

Our derivation of the driving potential that accelerates adiabatic population transfer in a lattice reveals a striking difference between a lattice system and a continuous system. Specifically, in the lattice system there is a lower limit to T_F. This limit derives from the condition for the additional phase in Eq. (5), which gives the lower limit for $\dot{R}$ for each R depending on $\phi_n(R)$, that is, trajectory of the evolution of the system. We believe that the accelerated population transfer scheme described in this paper can be used for the coherent control of many quantum systems which are described by chain or lattice models.

ACKNOWLEDGMENT

S.M. thanks Grants-in-Aid for Centric Research of Japan Society for Promotion of Science and JSPS Postdoctoral Fellowships for Research Abroad for its financial support.

APPENDIX: ACCELERATION OF NONADIABATIC DYNAMICS

We consider the acceleration of nonadiabatic quantum dynamics. Consider the wave function $\Psi(m,t)$, which is a solution of a discrete time-dependent Schrödinger equation:

$$i\frac{d\Psi(m,t)}{dt} = \sum_l \omega_{m,l}\Psi(l,t) + \frac{V(m,t)}{\hbar}\Psi(m,t). \tag{A1}$$

We seek a driving potential that generates the target state $\Psi(m,T)$ at $t = T_F(<T)$. We assume that the wave function

of the intermediate state is

$$\Psi_{\rm FF}(m,t) = \Psi(m,\Lambda(t))e^{if(m,t)}, \tag{A2}$$

where $f(m,t)$ is the additional phase and

$$\Lambda(t) = \int_0^t \alpha(t')dt'. \tag{A3}$$

α is a real function of time called magnification factor [15]. The time dependence of α is chosen so that it satisfies

$$\Lambda(T_F) = T. \tag{A4}$$

We assume that $\Psi_{\rm FF}(m,t)$ is a solution of the Schrödinger equation:

$$i\frac{d\Psi_{\rm FF}(m,t)}{dt} = \sum_l \omega_{m,l}\Psi_{\rm FF}(m,t) + \frac{V_{\rm FF}(m,t)}{\hbar}\Psi_{\rm FF}(m,t), \tag{A5}$$

where $V_{\rm FF}$ is the driving potential. Following the same analysis as in Sec. II, we find

$$\alpha(t)\sum_l {\rm Im}[\omega_{m,l}\Psi_m^*\Psi_l] = \sum_l {\rm Im}\{\omega_{m,l}\Psi_m^*\Psi_l \exp[i(f_l - f_m)]\} \tag{A6}$$

and

$$V_{\rm FF}(m,t) = \sum_l {\rm Re}\left\{\frac{\hbar\omega_{m,l}\Psi_l}{\Psi_m}[\alpha(t) - e^{i(f_l - f_m)}]\right\} + \alpha(t)V(m,\Lambda(t)) - \hbar\partial_t f_m, \tag{A7}$$

where f_m and Ψ_m are abbreviations for $f(m,t)$ and $\Psi(m,\Lambda(t))$, respectively. Equation (A6) is used to obtain the additional phase. The driving potential is obtained by substitution of f_m into Eq. (A7). As in the case of acceleration of adiabatic population transfer, there is a lower limit to T_F because Eq. (A6) gives the upper limit of $\alpha(t)$ for each t. The equations for f and $V_{\rm FF}$ in Eqs. (A6) and (A7) reduce to those for continuous systems in Ref. [15] in the limit that the differences in $f(m,t)$ and $\Psi(m,t)$ between adjacent sites are small.

[1] S. A. Rice and M. Zhao, *Optical Control of Molecular Dynamics* (Wiley, New York, 2000).
[2] M. Shapiro and P. Brumer, *Principles of the Quantum Control of Molecular Processes* (Wiley, New York, 2003).
[3] T. Baumert, B. Bühler, R. Thalweiser, and G. Gerber, Phys. Rev. Lett. **64**, 733 (1990).
[4] U. Gaubatz, P. Rudecki, S. Schiemann, and K. Bergmann, J. Chem. Phys. **92**, 5363 (1990).
[5] T. Baumert, M. Grosser, R. Thalweiser, and G. Gerber, Phys. Rev. Lett. **67**, 3753 (1991).
[6] P. Dittmann, F. P. Pesl, J. Martin, G. W. Coulston, G. Z. He, and K. Bergmann, J. Chem. Phys. **97**, 9472 (1992).
[7] T. Halfmann and K. Bergmann, J. Chem. Phys. **104**, 7068 (1996).
[8] J.-F. Schaff, X.-L. Song, P. Vignolo, and G. Labeyrie, Phys. Rev. A **82**, 033430 (2010).
[9] J.-F. Schaff, X.-L. Song, P. Capuzzi, P. Vignolo, and G. Labeyrie, Eur. Phys. Lett. A **93**, 23001 (2011).
[10] M. G. Bason, M. Viteau, N. Malossi, P. Huillery, E. Arimondo, D. Ciampini, R. Fazio, V. Giovannetti, R. Mannella, and O. Morsch, Nat. Phys. **8**, 147 (2011).
[11] M. Demirplak and S. A. Rice, J. Phys. Chem. **107**, 9937 (2003).
[12] M. V. Berry, J. Phys. A **42**, 365303 (2009).
[13] K. Takahashi, Phys. Rev. E **87**, 062117 (2013).
[14] J. G. Muga, X. Chen, A. Ruschhaupt, and D. Guéry-Odelin, J. Phys. B **42**, 241001 (2009).
[15] S. Masuda and K. Nakamura, Phys. Rev. A **78**, 062108 (2008).
[16] S. Masuda and K. Nakamura, Proc. R. Soc. A **466**, 1135 (2010).
[17] S. Masuda and K. Nakamura, Phys. Rev. A **84**, 043434 (2011).
[18] S. Masuda, Phys. Rev. A **86**, 063624 (2012).
[19] E. Torrontegui, X. Chen, M. Modugno, S. Schmidt, A. Ruschhaupt, D. Guéry-Odelin, and J. G. Muga, New J. Phys. **14**, 013031 (2012).
[20] S. Masuda, Phys. Rev. A **88**, 013625 (2013).
[21] O. Morsch and M. Oberthaler, Rev. Mod. Phys. **78**, 179 (2006).
[22] T. C. H. Liew and I. A. Shelykh, J. Phys. B: At. Mol. Opt. Phys. **45**, 245003 (2012).
[23] A. Trombettoni and A. Smerzi, Phys. Rev. Lett. **86**, 2353 (2001).
[24] F. S. Cataliotti, S. Burger, C. Fort, P. Maddaloni, F. Minardi, A. Trombettoni, A. Smerzi, and M. Inguscio, Science **293**, 843 (2001).